# Role of unsaturated hydrocarbon lubricant on the friction behavior of amorphous carbon films from reactive molecular dynamics study

Xiaowei Li[a,b,*], Aiying Wang[a], Kwang-Ryeol Lee[b,*]

[a] Key Laboratory of Marine Materials and Related Technologies, Zhejiang Key Laboratory of Marine Materials and Protective Technologies, Ningbo Institute of Materials Technology and Engineering, Chinese Academy of Sciences, Ningbo 315201, PR China
[b] Computational Science Center, Korea Institute of Science and Technology, Seoul 136-791, Republic of Korea

## ARTICLE INFO

## ABSTRACT

Compositing amorphous carbon (a-C) film with fluid lubricant could successfully improve the friction properties and prolong the service life and reliability of protected components. However, the inevitable existence of unsaturated molecules in base oil, especially its potential effect on the friction behavior and related mechanism are still not fully understood. In this paper, the friction behavior of amorphous carbon (a-C) composited with unsaturated hydrocarbon lubricant, $C_5H_{10}$ as one of linear alpha olefins (AO), was explored by reactive molecular dynamics simulation, and the role of $C_5H_{10}$ content on friction property and interfacial structure was mainly analyzed. Results revealed that at the fixed contact pressure, the unsaturated $C_5H_{10}$ bound with a-C in the form of weak intermolecular interactions rather than chemical bonding and there was also no $C_5H_{10}$ dissociation observed; the friction coefficient was strongly dependent on the small unsaturated hydrocarbon, which decreased obviously with $C_5H_{10}$ content. In particular, compared to the dry condition, the existence of $C_5H_{10}$ molecules at the friction interface could significantly reduce the friction coefficient by 99.2% maximally. By the systematical analysis of interfacial hybridization structure and AO mobility, it indicated that the synergistic mechanism for the low friction originated from the self-passivation of a-C surface and AO hydrodynamic lubrication. Our results not only disclose the effect of unsaturated hydrocarbon molecules in bas oil on friction behavior and define the underlying lubrication mechanism, but also suggest a strategy for the design of both fluid lubricant and friction interface to realize the long-lifetime application.

## 1. Introduction

The key mechanical components of automobile, such as tappet, injection nozzle for diesel engines, etc., face high challenges and requirement for wear resistance and friction properties in order to avoid the global environmental destruction and resource depletion. Amorphous carbon (a-C) film, due to its high hardness, low friction coefficient and chemical inertness, has been a strong candidate as a protective coating for automobile application against serious mechanical or chemical damage [1–4]. In particular, the limitations of intrinsic a-C film, such as high residual compressive stress [1,4], poor adhesion strength to metal substrate [3], and environment-dependent wear properties [5], have been greatly improved until now by doping metal element into a-C structure [6,7], the introduction of interlayer and multilayer structure fabrication [8,9]. However, no matter how low the friction coefficient could achieve [10], the efficiency of antifriction property induced by a-C film is always operated at expense of its self-consumption, which restricts its lifetime and reliability seriously for wider applications in the automobile industry.

Recently, many efforts have indicated that by the combination of a-C film and alpha-olefin (AO)-based lubricant oil, the friction reducing and antiwear abilities of mechanical moving components could be improved successfully for the long-lifetime and reliability service [11–13]. For example, Kano [11] obtained the super low friction coefficient of 0.006 by the material combination of the steel pin/a-C disc pair lubricated with the ester containing poly alpha olefin (PAO) oil at the boundary lubrication condition, and large friction reduction of more than 45% could be realized at an engine speed of 2000 rpm. Jia et al. [12] found that the PAO oil functionalized by borate esters additive was effective in significantly increasing the friction-reduction and wear resistance properties for a-C/steel and a-C/a-C sliding pairs. The abovementioned results show that the friction properties of a-C film could be further modified by lubricating with PAO oil.

As well known that there are unsaturated AO molecules inevitably

* Corresponding authors at: Computational Science Center, Korea Institute of Science and Technology, Seoul 136-791, Republic of Korea (X. Li).
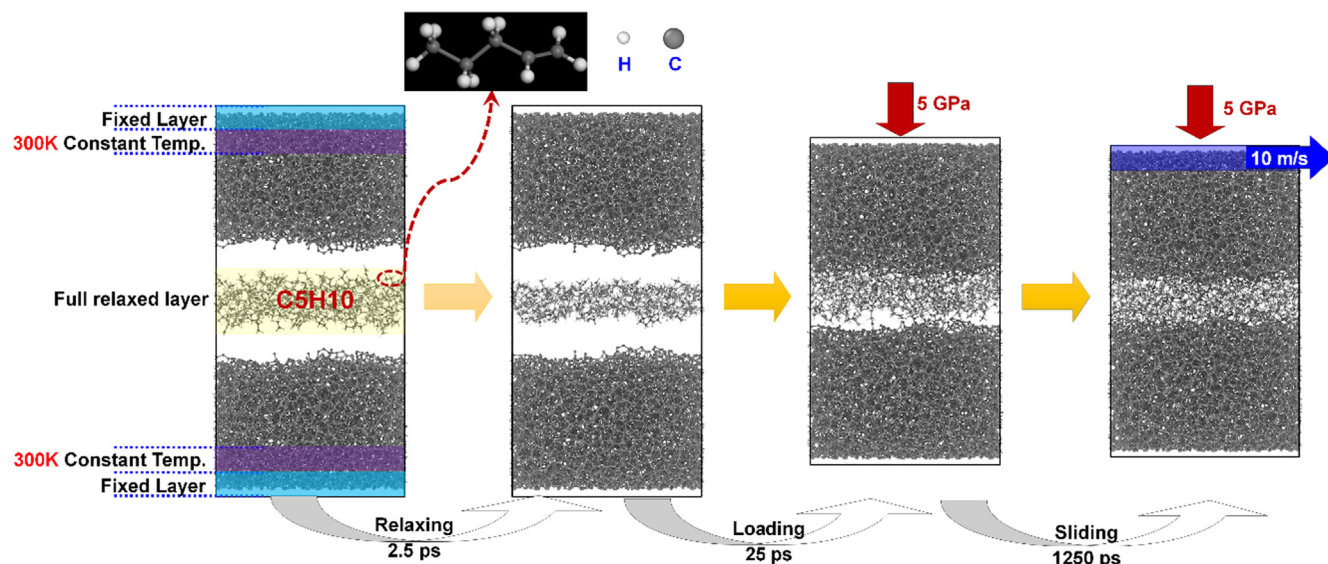E-mail addresses: lixw0826@gmail.com (X. Li), krlee@kist.re.kr (K.-R. Lee).

**Fig. 1.** Friction simulation model of a-C/$C_5H_{10}$/a-C system and related parameters.

existed in PAO oil, which are more reactive than saturated cases. However, the interaction of unsaturated AOs with a-C was seldom gave much attention. In particular, Erdemir [14] reported that the unsaturated species in PAO oil, which promoted the *operando* formation of carbon-based tribofilms as solid lubricant via dissociative extraction from themselves, played an important role on the improvement of friction behavior. The in-depth investigation on the adsorption and bonding state of unsaturated AOs with a-C and its dependence on the variety and content of AOs and the contact pressure, especially the corresponding structural evolution of friction interface, is required, which is essential to unveil the underlying friction mechanism and drive the effective development of new lubricant system. In addition, there is few published work on friction interaction between the a-C and AO lubricant from atomic scale using ReaxFF [15,16], which can give more accurate description for the complicated structural transformation of carbon-carbon interaction than previous Tersoff [17,18], REBO [19], and AIREBO [20] potentials.

In our recent studies [21,22], we have systematically investigated the bonding and dissociation of AOs on its variety and contact pressure, indicating that although the unsaturated AOs were unstable, their dissociation induced by high contact pressure could passivate the sliding interface of a-C, contributing to the low friction behavior. So in the present work, we selected pentene, $C_5H_{10}$, as the represented unsaturated linear AO lubricant and mainly explored the dependence of friction behavior of a-C/$C_5H_{10}$/a-C system on $C_5H_{10}$ content by the reactive molecular dynamics (MD) simulation. Similar to previous study [23], hydrogen was also neglected from a-C structure in order to exclude its effect on not only the deterioration of mechanical properties of intrinsic a-C but also the real nature of friction in intrinsic a-C films. ReaxFF developed by Srinivasan [15] and Tavazza [16] was used to describe the C–C, C–H, and H–H interactions. The effect of $C_5H_{10}$ content on the friction property of a-C film was evaluated, and the interfacial structure evolution was mainly focused on to reveal the role of unsaturated AOs and fundamental friction mechanism. Results revealed that the friction property strongly depended on the unsaturated $C_5H_{10}$ content; the ultra-low friction was inspired by the synergistic effect from the self-passivation of a-C surface and $C_5H_{10}$ hydrodynamic lubrication.

## 2. Computational details

### 2.1. Model fabrication and parameters

The Large-scale Atomic/Molecular Massively Parallel Simulator (LAMMPS) code [24] was adopted for the reactive MD simulation of a-C/$C_5H_{10}$/a-C system. Fig. 1 showed the model used in the calculations. The a-C with size of $42.88 \times 40.358 \times 31$ Å$^3$ was produced by atom-by-atom deposition [25] and was set as the bottom and upper mating materials, which was composed of 6877 carbon atoms and had the sp$^3$C fraction of 24 at.% and density of 2.7 g/cm$^3$. For each a-C structure, it was divided into three layers including the fixed layer with thickness of 5 Å for mimicking the semi-infinite large surface, thermostatic layer with thickness of 5 Å for providing a thermal reservoir to the simulation system and free layer with thickness of 21 Å for simulating the structural evolution during the friction process (Fig. 1). The $C_5H_{10}$ lubricant was located at the central position, whose surface was 3 Å from the bottom or upper a-C film, and the number of molecules ranged from 32 to 72 and 122 separately in order to study the effect of $C_5H_{10}$ content on the friction property. Periodic boundary condition was employed along $x$ and $y$ directions, and a MD time step of 0.25 fs was used.

Before the friction process, the a-C/$C_5H_{10}$/a-C system was first relaxed at 300 K for 2.5 ps using *NVE* ensemble with Berendsen thermostat [26], and then the contact pressure of 5 GPa was loaded to the system during 25 ps. The corresponded changes of density and co-ordination number along the z direction after each step could be found in Fig. S1 of Supporting Information. After that, the sliding process began by exerting the sliding velocity of 10 m/s along the $x$ direction on the upper fixed a-C layer, and the sliding process lasted 1250 ps for each case to get the steady-state friction stage. After friction process, the friction coefficient, μ, was calculated using the following equation:

$$\mu = \frac{f}{W} \tag{1}$$

where the frictional force, $f$, and the normal force, $W$, were calculated by summing the force acting on the fixed atoms of bottom a-C layer in the $x$ and $z$ directions, respectively.

It should be mentioned that for the contact pressure (5 GPa) used in the present work, it seemed to be much higher than that in experiment. On the one hand, many reports [27–30] exhibited that the high contact pressure could be possible for instantaneous contact of a-C asperities during friction process, and it was also appropriate for examining the friction behavior on an atomic scale. On the other hand, when the
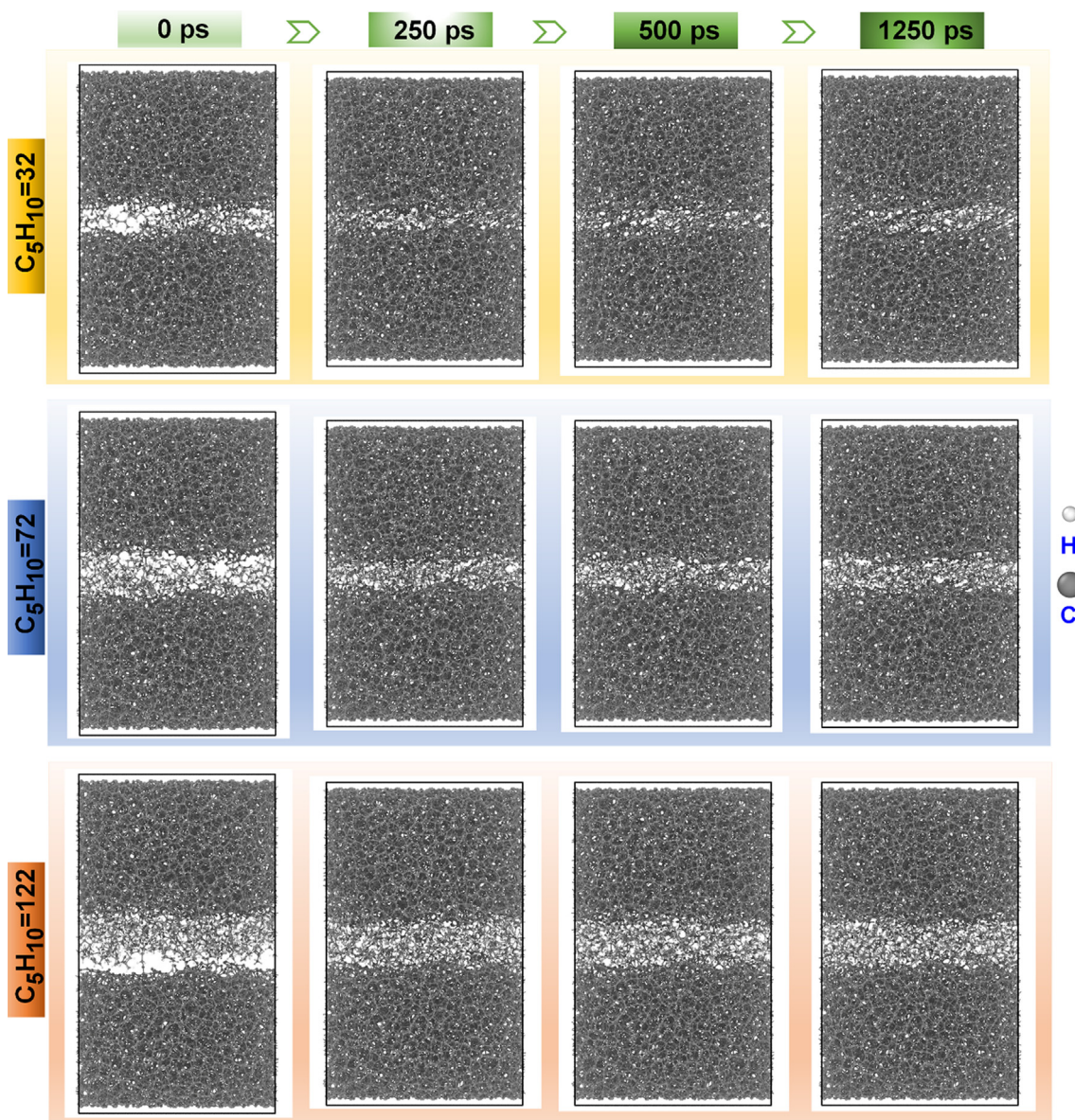
**Fig. 2.** Morphologies of a-C/$C_5H_{10}$/a-C friction systems with different $C_5H_{10}$ contents.

contact pressure was 5 GPa, the generated normal force value (about 38 nN) was much smaller than 120 nN obtained under 1 GPa in previous study [31], which attributed to the difference in surface state (hybridization, adatom passivation, and roughness) of a-C films; if the contact pressure reduced to 1 and 0.5 GPa, there was almost no interaction between the mating materials (see Fig. S2 of Supporting Information) due to the neglectable normal forces, which was similar to previous work [32]. In addition, the sliding velocity was also higher than that in experiment due to the limitation of short MD simulation time [33], whose applicability has been confirmed by previous studies [31,34,35].

### 2.2. ReaxFF validation

ReaxFF force field [15,16] was used to describe the C–C, C–H and H–H interactions in the system. Although it has been confirmed to model the covalent bond forming and breaking, rehybridization, and chemical reactions accurately in carbon-based structures, the additional evaluations for the formation energy of $C_5H_{10}$ under different temperatures, the adsorption energy of $C_5H_{10}$ on a-C surface, and the a-C structure fabrication using quenching method were further performed

by ReaxFF MD and ab-initio calculations [36,37] separately, and the MD calculations for a-C growth by atom-by-atom method was also conducted using ReaxFF and AIREBO potentials [20], respectively. These results clearly verified the validity and reliability of the force field for our simulated system [21–23].

### 3. Results and discussion

Fig. 2 shows the morphology evolution of a-C/$C_5H_{10}$/a-C friction systems with different $C_5H_{10}$ contents during the friction process. It can be seen that with the sliding time ranged from 0 to 1250 ps, the atoms from a-C and $C_5H_{10}$ lubricant interact with each other to form the stable friction interface, and $C_5H_{10}$ molecules tend to be distributed along the sliding direction. However, when the number of $C_5H_{10}$ molecules increases from 32 to 72 and 122, the two a-C/$C_5H_{10}$ interfaces can be distinguished clearly, and most of $C_5H_{10}$ molecules exist in the central position between the bottom and upper mating a-C materials without interacting with a-C structures. This may attribute to the low contact pressure of 5 GPa, which cannot provide the enough driving force or energy for uniform mixing [21].

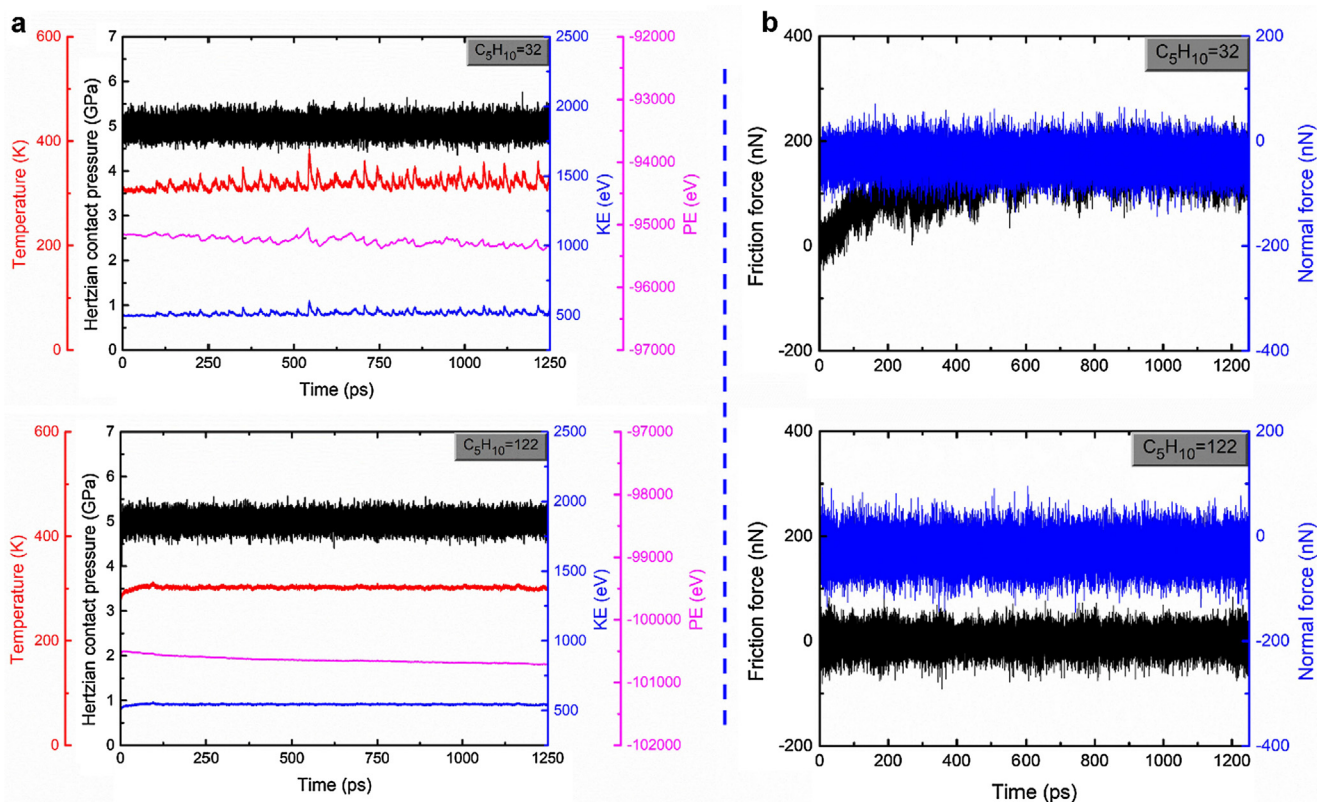During the friction process, the contact pressure, temperature, and

**Fig. 3.** (a) Contact pressure, temperature, KE and PE energies and (b) friction force and normal force with sliding time in a-C/$C_5H_{10}$/a-C friction systems with 32 and 122 $C_5H_{10}$ molecules, respectively.
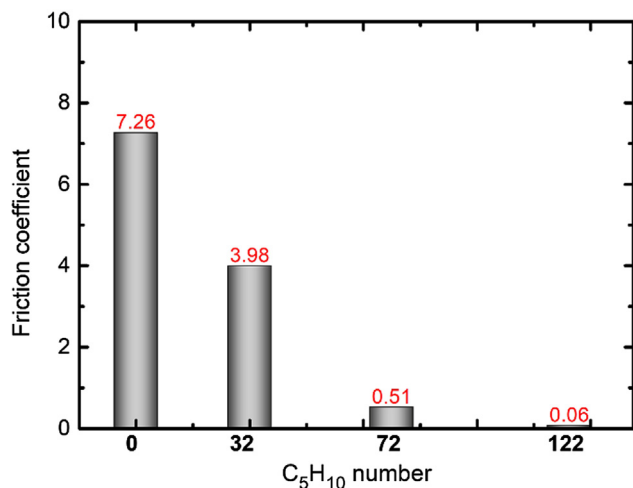


**Fig. 4.** Friction coefficient as a function of $C_5H_{10}$ content. The result in pure a-C/a-C without lubricant system is also considered for comparison.

energies including kinetic energy (KE) and potential energy (PE) with sliding time are given in Fig. 3a, and the result for the system with $C_5H_{10}$ number of 72 can be found in previous study [21]. Compared to the dry condition (see Fig. S3 in Supporting Information), the evolutions of both the energy and temperature at the sliding interface confirm that under the $C_5H_{10}$ condition, the system only takes shorter time for running-in process to reach the stable friction stage, and the time further decreases with $C_5H_{10}$ content. In addition, when the number of $C_5H_{10}$ increases from 32, 72 to 122, the fluctuations of temperature, KE, and PE with $C_5H_{10}$ content are smoothed due to the decreased interaction between the two a-C surfaces separated by the $C_5H_{10}$ lubricant (Fig. 2). At the stable friction stage, the average temperatures at the

sliding interface are 322 ± 11, 304 ± 3, and 302 ± 3 K, respectively, for each case. The flash temperature rise at the interface can be estimated by the following equation [38,39]

$$\Delta T = \frac{\mu W v}{8 a K_{a-C}} \qquad (2)$$

where $\Delta T$ is the flash temperature rise; $\mu$ is the friction coefficient; $W$ is the applied normal force; $v$ is the sliding velocity; $a$ is the contact radius of real contact area; $K_{a-C}$ is the thermal conductivities of a-C. It suggests that besides the sliding velocity, the friction force also contributes to the temperature rise at the sliding interface, as will be discussed later.

Fig. 3b shows both the friction and normal force curves with sliding time in a-C/$C_5H_{10}$/a-C friction systems. It also proves the time reduction for running-in process with $C_5H_{10}$ content and the sliding time of 1250 ps is enough for each a-C/$C_5H_{10}$/a-C system to reach the stable friction state. In order to evaluate the dependence of friction property on $C_5H_{10}$ content, the friction and normal forces from the last 200 ps of stable friction process are adopted to calculate the average values. Note that with the $C_5H_{10}$ number ranged from 32 to 72 and 122, the average friction force decreases from 149.3 ± 34 to 19.4 ± 31 and 1.9 ± 27 nN, which can explain for the difference in temperature rise (Fig. 3a) at sliding interface according to Eq. (2). The friction coefficient as a function of $C_5H_{10}$ content is further evaluated according to Eq. (1), as illustrated in Fig. 4. The result in pure a-C/a-C system without lubricant is also considered for comparison. It shows that the friction coefficient with $C_5H_{10}$ content decreases significantly; when the number of $C_5H_{10}$ is 122, the minimal friction coefficient is only 0.06. However, it should be noted that the friction coefficient values in Fig. 4 are larger than those in experiment due to the strong adhesive strength between the two pure a-C friction surfaces which have no any passivation or contamination [33,40] and the inaccurate quantification of real contact area in experiment, but they are still comparable to the previous simulation result [41]. Furthermore, by comparison with the a-C/a-C
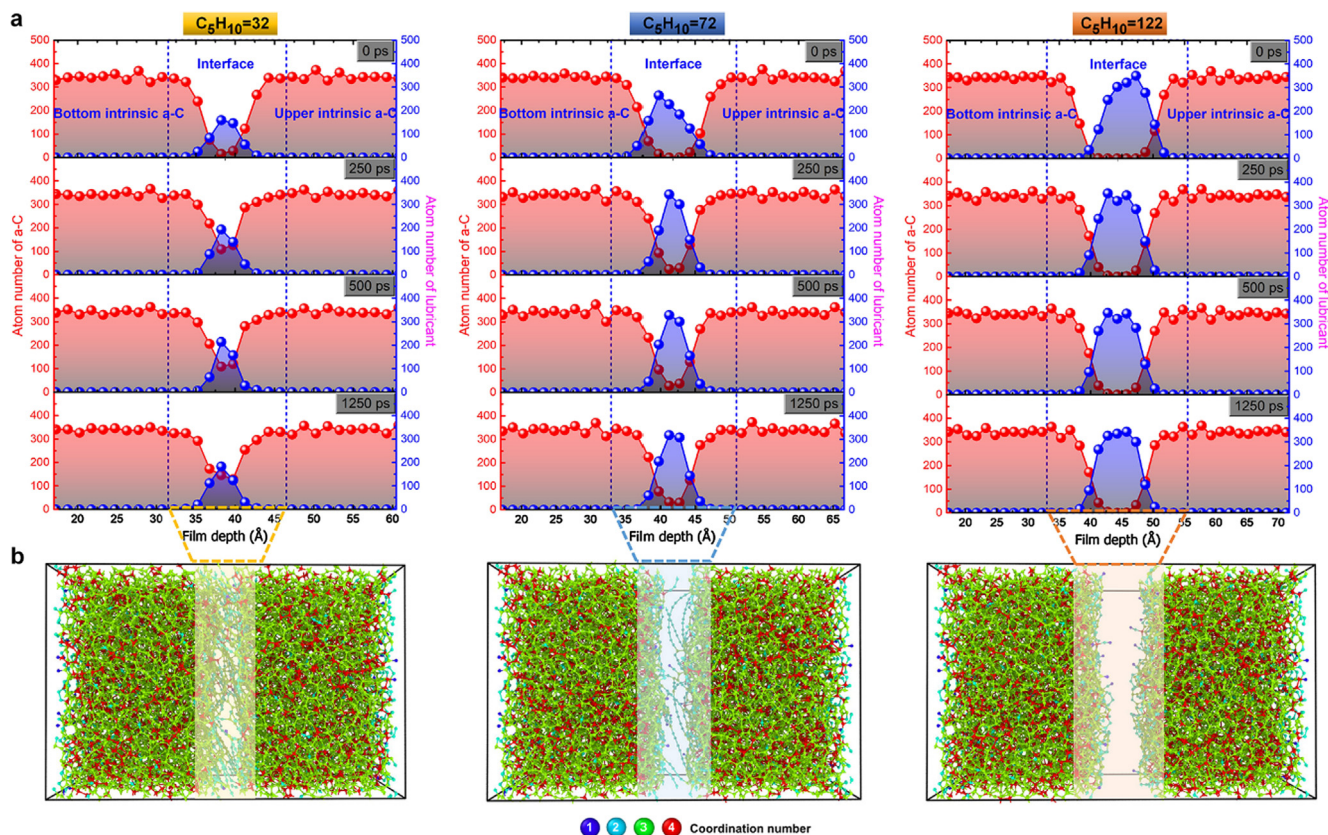
**Fig. 5.** (a) Atom distribution of a-C and lubricant along z direction in a-C/C$_5$H$_{10}$/a-C system with different C$_5$H$_{10}$ contents. (b) Final morphologies after the friction process for each case, in which the C$_5$H$_{10}$ molecules are neglected for convenient view.
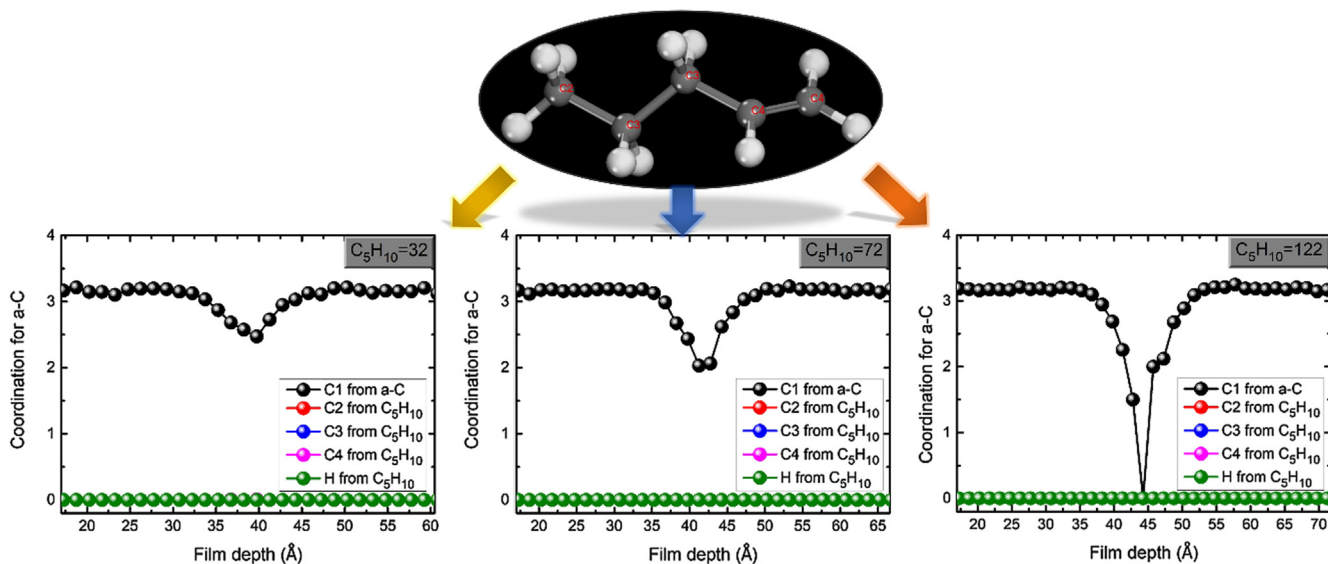


**Fig. 6.** Coordination of a-C structure contributed by a-C and C$_5$H$_{10}$ lubricant, respectively, in a-C/C$_5$H$_{10}$/a-C system with different C$_5$H$_{10}$ contents.

system without C$_5$H$_{10}$ lubricant, the addition of C$_5$H$_{10}$ could improve the friction property significantly and the maximal reduction of 99.2% for friction coefficient is achieved, which is also in agreement with previous report [13].

The evolutions of structure and property at the interface are closely related with the friction behavior, which is requisite to explore the friction mechanism caused by C$_5$H$_{10}$ lubricant. Before that, the atom distributions of a-C and lubricant along z direction in a-C/C$_5$H$_{10}$/a-C system is evaluated first for each case, as given in Fig. 5a. As can be seen

that the whole system can be divided into three regions including interfacial, bottom and upper intrinsic a-C layers for each case. At the two intrinsic a-C layers, the atom distribution almost has no change with sliding time, implying that the friction behavior mainly occurs at the interface. On the contrary, at the interfacial layer, the atoms from a-C and C$_5$H$_{10}$ mix with each other to form the stable interfacial layer gradually, and the width of interfacial layer with C$_5$H$_{10}$ content increase. However, due to the low contact pressure, when the number of C$_5$H$_{10}$ molecules is 72, there is a C$_5$H$_{10}$ plateau region with width of 3 Å
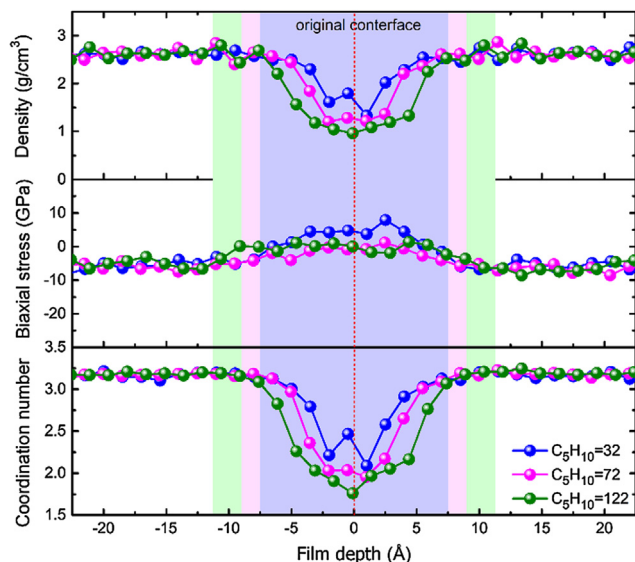
**Fig. 7.** Change of structural properties along z direction in a-C/C$_5$H$_{10}$/a-C system with different C$_5$H$_{10}$ contents after friction process, in which blue, pink and green colors represent the width of interfacial layer when the number of C$_5$H$_{10}$ molecules is 32, 72 and 122, respectively.

observed [21], and with further increasing the C$_5$H$_{10}$ number to 122, the plateau width reaches to 4.5 Å. This indicates that there are C$_5$H$_{10}$ molecules existed at the interface stably without interacting with a-C structures, which may have important effect on the friction behavior. Fig. 5b further shows the final morphologies after the friction process for each case, in which the C$_5$H$_{10}$ molecules are neglected for convenient viewing. It clearly reveals that when the number of C$_5$H$_{10}$ molecules is 32, the lubricant cannot fully cover the a-C surface, leading to the obvious inter-film bonding between the two mating a-C structures, which exist in the form of chain structures; however, with increasing the C$_5$H$_{10}$ to 122, the bottom and upper a-C surfaces can be separated completely without any direct inter-film interaction, suggesting the high mobility of C$_5$H$_{10}$ molecules.

In order to further define the binding state between the a-C and C$_5$H$_{10}$ lubricant, the coordination number of a-C structure contributed by a-C and C$_5$H$_{10}$ lubricant separately in a-C/C$_5$H$_{10}$/a-C system is further analyzed for each case, as shown in Fig. 6. It displays that under the different C$_5$H$_{10}$ contents, the C$_5$H$_{10}$ molecules make no contribution to the coordination number of a-C structures, indicating that the C$_5$H$_{10}$ molecules adsorb on the a-C surface in the form of intermolecular

interaction, rather than the chemical bonding due to low contact pressure [21] or the lack of catalytic metal at the friction surface [14]. Therefore, the contribution of a-C and C$_5$H$_{10}$ to friction coefficient can be considered, respectively.

Fig. 7 shows the change of structural properties along z direction in a-C/C$_5$H$_{10}$/a-C system with different C$_5$H$_{10}$ contents after friction process. The residual biaxial stress is also calculated according to the equations in previous report [42]. Based on the analysis in Fig. 5, under the different C$_5$H$_{10}$ contents, there is almost no change for the structural properties at the bottom and upper intrinsic a-C layers (white color in Fig. 7), while the significant evolution happen at the interface. With the number of C$_5$H$_{10}$ molecules ranged from 32 to 72 and 122, the widths of interfacial layer are 15 (blue color), 18 (pink color) and 22.5 Å (green color), respectively, which are used to calculate the density, residual stress, and hybridization structures of interface after the friction process, as given in Figs. 8 and 9. For comparison, the result in a-C/a-C system without lubricant is also given. First, Fig. 8 reveals that compared to the pure case without lubricant, the addition of C$_5$H$_{10}$ lubricant reduces the density at the interface, while the compressive stress increases because the C$_5$H$_{10}$ lubricant as barrier layer prohibit the formation of chain-like carbon structures at the sliding interface (Fig. 5b). Following the increase of C$_5$H$_{10}$ content, the density contributed by a-C decreases gradually, while the compressive stress increases first and then decreases slightly, which is mainly affected by the complicated interactions between the bottom and upper a-C surfaces or a-C and C$_5$H$_{10}$ lubricant. For the contribution from C$_5$H$_{10}$ lubricant, the density as a function of C$_5$H$_{10}$ content increases, which is contrary to the change of compressive stress.

Because there is no chemical bonding between the a-C surface and C$_5$H$_{10}$, the hybridization structure of C$_5$H$_{10}$ must have no change, so the change of a-C hybridization structure at the interface is mainly analyzed, as shown in Fig. 9. First, by comparison with the original interface (sp$^2$C fraction-62.9 at.%) before sliding process, the friction-induced increase of sp$^2$C fraction is achieved for each case, which is in accordance with the early experimental work [13]. However, compared to the pure a-C/a-C system without C$_5$H$_{10}$, introducing C$_5$H$_{10}$ lubricant into a-C/a-C system could reduce the sp$^2$C fraction, while the sp$^3$C fraction increase, which results from the increased compressive stress (Fig. 8) according to the pressure-temperature (P-T) phase diagram for carbon [43,44]. The highly compressive stress favors the formation of a sp$^3$C-rich phase, while a tensile one favors a sp$^2$C-rich phase [23]. As the number of C$_5$H$_{10}$ molecules changes from 32 to 72 and 122, both the sp$^2$C and spC fractions decrease following the increase of sp$^3$C fraction (Fig. 9a), while the s-hybridized contribution can be neglected due to low fraction. Hence, the decrease of un-passivated bonds of a-C surface including sp$^2$C and spC with C$_5$H$_{10}$ content weakens the
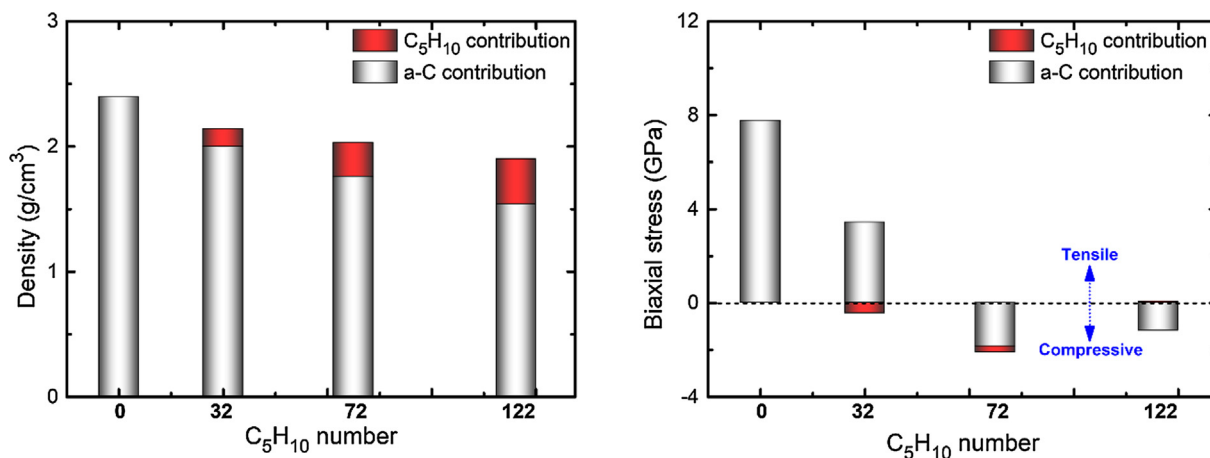


**Fig. 8.** C$_5$H$_{10}$ content dependence of density and stress of interface contributed by a-C and C$_5$H$_{10}$, respectively, after the friction process. The result in pure a-C/a-C system without lubricant is also considered for comparison.
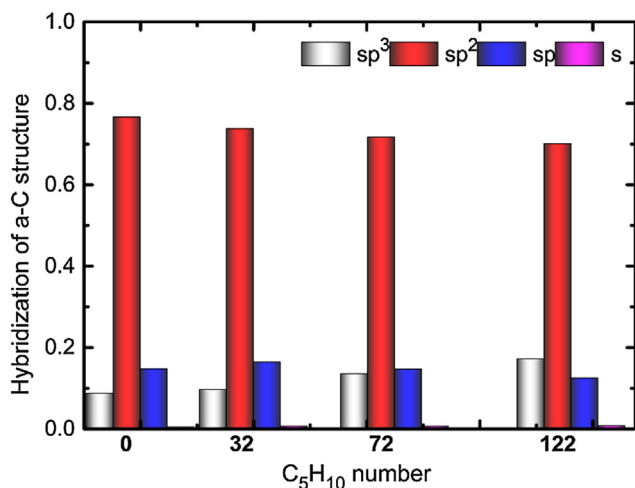
**Fig. 9.** Hybridization structure of a-C at the interface as a function of $C_5H_{10}$ content after friction process. The result in pure a-C/a-C system without lubricant is also considered for comparison.
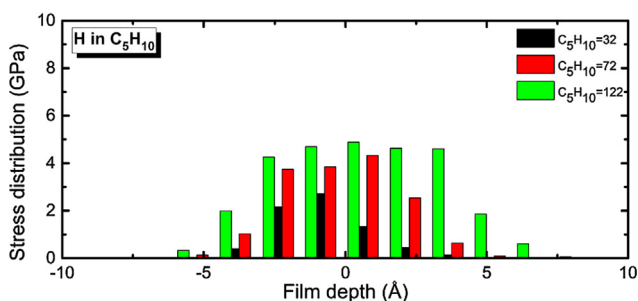


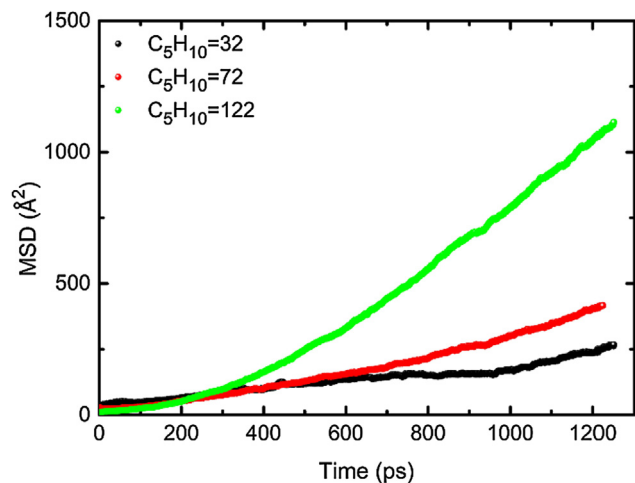**Fig. 10.** Stress distribution of H atoms along film depth direction in $C_5H_{10}$ lubricant.



**Fig. 11.** MSD of $C_5H_{10}$ molecules along x direction in the a-C/$C_5H_{10}$/a-C systems.

interaction between the $C_5H_{10}$ and a-C structure, contributing to the low friction coefficient shown in Fig. 4, which is similar to previous reports [23]. This provides straightforward evidence for the effect of interfacial passivation on friction, which is estimated by Cui et al. [38] due to the limited characterization technique. However, it should be noted that the H atoms in the lubricant, especially those at the a-C/$C_5H_{10}$ interface, exhibit the repulsive force [30], as shown in Fig. 10, and the force value increases obviously with the $C_5H_{10}$ content, which also makes contribution to the self-passivation of a-C surface.

Most importantly, because there is no chemical bonding between the a-C and $C_5H_{10}$ molecules, the mobility of $C_5H_{10}$ molecules in the friction system is evaluated approximately by the mean-square displacement (MSD), which is estimated as follows:

$$\text{MSD} = r^2(t) = \frac{1}{N} \left\langle \sum_{i=1}^{N} |r_i(t) - r_i(0)|^2 \right\rangle \tag{3}$$

where $N$ is the number of $i$ atoms in the system, and $r_i(t)$ is the position of the $i$ atom at $t$ moment and $r_i(0)$ is the position of the $i$ atom at $t = 0$ moment. Fig. 11 shows the MSD of $C_5H_{10}$ molecules along x direction in the a-C/$C_5H_{10}$/a-C systems. It can be seen that with the number of $C_5H_{10}$ molecules, the MSD increases significantly due to the significant reduction of C–C inter-film bonding interaction from both a-C films (Fig. 5a) and the passivation of carbon dangling bonds at the a-C surface (Fig. 9). This suggests the enhanced mobility along the sliding direction with $C_5H_{10}$ content, which should make the main contribution to the low friction coefficient because of the weak intermolecular interaction between the a-C and $C_5H_{10}$. Fig. 12 further gives the dependence of shearing strength on $C_5H_{10}$ content, which is calculated as following

$$\mu = \frac{S}{\sigma} \tag{4}$$

where $S$ is the shearing strength, $\sigma$ is the Hertzian contact pressure, which is 5 GPa in this calculation. Under dry condition, the shearing strength is 36.3 GPa, while it decreases to 19.9, 2.6 and 0.3 GPa, respectively when the number of $C_5H_{10}$ molecules increases to 32, 72 and 122. Therefore, the combined effect from the self-passivation of a-C surface and $C_5H_{10}$ hydrodynamic lubrication reduces the shearing strength between the mating friction surfaces significantly, accounting for the friction behavior of a-C system composited with $C_5H_{10}$ lubricant.

It should be mentioned that if the H-, F-, or O-passivated a-C are introduced instead of the intrinsic a-C in this study, the friction behavior should be further improved due to the passivation of a-C surface following the enhanced mobility of AO lubricant. Although this work clarifies the role of unsaturated AO molecules on friction behavior of a-C and underlying friction mechanism and provides a clue to modify the passivation state of sliding interface and lubrication effectiveness by controlling the content of unsaturated hydrocarbon molecules in PAO, the direct comparison between the simulation and experimental results is still a big challenge until now due to the limitations in the simplified contact model without multiple asperities, friction parameters (time, sliding velocity, contact pressure, and environment), the hybridization and surface state of a-C structure as observed in experiment, etc.

## 4. Conclusions

In this study, we performed reactive MD simulation using ReaxFF force field to investigate the effect of unsaturated $C_5H_{10}$ on friction behavior of a-C/a-C system, and the dependence of friction property and interfacial structure evolution on $C_5H_{10}$ content was mainly studied. In order to explore the related friction mechanism, the hybridization structure, density, residual stress, and friction coefficient were calculated. Results revealed that the unsaturated $C_5H_{10}$ content played a significant role on the friction coefficient, which decreased significantly as a function of the $C_5H_{10}$ content, and the minimal friction coefficient of 0.06 was obtained when the number of $C_5H_{10}$ molecules was 122. By comparison with the pure case without $C_5H_{10}$ lubricant, the addition of $C_5H_{10}$ could reduce the friction coefficient by 99.2% maximally. Moreover, the $C_5H_{10}$ molecules bind with a-C by intermolecular interaction, rather than the chemical bonding due to the relative low contact pressure. By analyzing the hybridization structure of a-C and MSD result as a function of $C_5H_{10}$ content, it revealed that compared with the original interface before friction, although the increased sp$^2$ fraction could observed for each case after friction process,
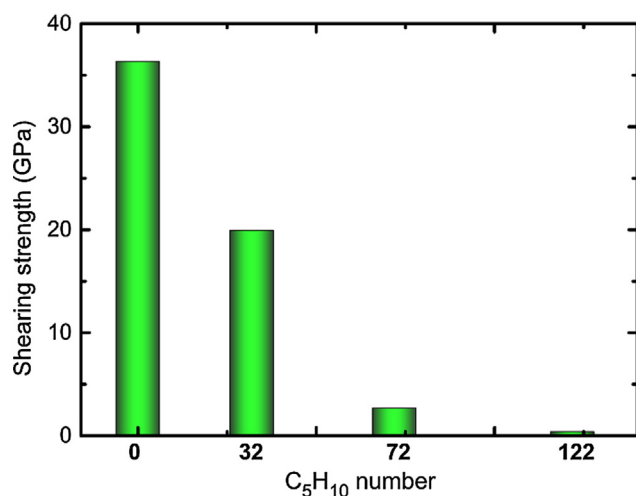
**Fig. 12.** Shearing strength as a function of $C_5H_{10}$ contents.

the transformation of interfacial stress from tensile state to compressive state and the repulsion force of H induced the self-passivation of a-C surface, and the hydrodynamic lubrication of small unsaturated AOs was also promoted by the significant reduction of a-C/a-C inter-film interaction, which could account for the excellent friction property and also provide the scientific understanding for AO's role in the a-C friction system.

## Data availability

The authors declare that the data supporting the findings of this study are available within the paper and its Supporting information file.

## CRediT authorship contribution statement

**Xiaowei Li:** Conceptualization, Methodology, Software, Validation, Investigation, Writing - original draft, Writing - original draft, Writing - review & editing, Funding acquisition. **Aiying Wang:** Conceptualization, Writing - review & editing, Funding acquisition. **Kwang-Ryeol Lee:** Conceptualization, Methodology, Resources, Investigation, Writing - review & editing, Supervision, Funding acquisition.

## Acknowledgments

## Appendix A. Supplementary data

Density and coordination change along the z direction after loading process for each case (Fig. S1); Simulation results under the contact pressures of 1 and 0.5 GPa, respectively (Fig. S2); Contact pressure, temperature, KE and PE with sliding time in a-C/a-C friction system without $C_5H_{10}$ lubricant (Fig. S3). Supplementary data to this article can be found online at https://doi.org/10.1016/j.commatsci.2019.01.032.

## References

[1] W. Dai, J. Liu, D. Geng, P. Guo, J. Zheng, Q. Wang, Microstructure and property of diamond-like carbon films with Al and Cr co-doping deposited using a hybrid beams system, Appl. Surf. Sci. 388 (2016) 503–509.

[2] W. Dai, F. Liu, J.C. Ding, Q. Wang, S.H. Kwon, Amorphous carbon films with MoCu dual-doping deposited by a hybrid sputtering system, Diam. Relat. Mater. 87 (2018) 107–114.

[3] X. Chen, Z. Peng, Z. Fu, W. Yue, X. Yu, C. Wang, Influence of individual C-C layer thickness on structure and tribological properties of multilayered Cr-C/a-C: Cr Thin Films, Surf. Coat. Technol. 204 (2010) 3319–3325.

[4] W. Dai, X. Gao, J. Liu, Q. Wang, Microstructure, mechanical property and thermal stability of diamond-like carbon coatings with Al, Cr and Si multi-doping, Diam. Relat. Mater. 70 (2016) 98–104.

[5] J. Andersson, R.A. Erck, A. Erdemir, Friction of diamond-like carbon films in different atmospheres, Wear 254 (2003) 1070–1075.

[6] J. Huang, L. Wang, B. Liu, S. Wan, Q. Xue, In vitro evaluation of the tribological response of Mo-doped graphite-like carbon film in different biological media, ACS Appl. Mater. Interfaces 7 (2015) 2772–2783.

[7] X. Li, P. Guo, L. Sun, A. Wang, P. Ke, Ab initio investigation on Cu/Cr codoped amorphous carbon nanocomposite films with giant residual stress reduction, ACS Appl. Mater. Interfaces 7 (2015) 27878–27884.

[8] J. Wang, J. Pu, G. Zhang, L. Wang, Interface architecture for superthick carbon-based films toward low internal stress and ultrahigh load-bearing capacity, ACS Appl. Mater. Interfaces 5 (2013) 5015–5024.

[9] X. Li, L. Li, D. Zhang, A. Wang, Ab initio study of interfacial structure transformation of amorphous carbon catalyzed by Ti, Cr, and W transition layers, ACS Appl. Mater. Interfaces 9 (2017) 41115–41119.

[10] X. Liu, J. Yang, J. Hao, J. Zheng, Q. Gong, W. Liu, A near-frictionless and extremely elastic hydrogenated amorphous carbon film with self-assembled dual nanostructure, Adv. Mater. 24 (2012) 4614–4617.

[11] M. Kano, Super low friction of DLC applied to engine cam follower lubricated with ester-containing oil, Tribol. Int. 39 (2006) 1682–1685.

[12] Z. Jia, Y. Xia, J. Li, X. Pang, X. Shao, Friction and wear behavior of diamond-like carbon coating on plasma nitrided mild steel under boundary lubrication, Tribol. Int. 43 (2010) 474–482.

[13] H.A. Tasdemir, M. Wakayama, T. Tokoroyama, H. Kousaka, N. Umehara, Y. Mabuchi, T. Higuchi, Ultra-low friction of tetrahedral amorphous diamond-like carbon (ta-C DLC) under boundary lubrication in poly alpha-olefin (PAO) with additives, Tribol. Int. 65 (2013) 286–294.

[14] A. Erdemir, G. Ramirez, O.L. Eryilmaz, B. Narayanan, Y. Liao, G. Kamath, S.K.R.S. Sankaranarayanan, Carbon-based tribofilms from lubricating oils, Nature 536 (2016) 67–71.

[15] S.G. Srinivasan, A.C.T. van Duin, P. Ganesh, Development of a ReaxFF potential for carbon condensed phases and its application to the thermal fragmentation of a large fullerene, J. Phys. Chem. A 119 (2015) 571–580.

[16] F. Tavazza, T.P. Senftle, C. Zou, C.A. Becker, A.C.T. van Duin, Molecular dynamics investigation of the effects of tip-substrate interactions during nanoindentation, J. Phys. Chem. C 119 (2015) 13580–13589.

[17] J. Tersoff, New empirical approach for the structure and energy of covalent systems, Phys. Rev. B 37 (1988) 6991–7000.

[18] P. Erhart, K. Albe, Analytical potential for atomistic simulation of silicon, carbon, and silicon carbide, Phys. Rev. B 71 (2005) 035211.

[19] D.W. Brenner, O.A. Shenderova, J.A. Harrison, S.J. Stuart, B. Ni, S.B. Sinnott, A second-generation reactive empirical bond order (REBO) potential energy expression for hydrocarbons, J. Phys.: Condens. Matter 14 (2002) 783–802.

[20] S.J. Stuart, A.B. Tutein, J.A. Harrison, A reactive potential for hydrocarbons with intermolecular interactions, J. Chem. Phys. 112 (2000) 6472–6486.

[21] X. Li, A. Wang, K.R. Lee, Mechanism of contact pressure-induced friction at the amorphous carbon/alpha olefin interface, NPJ Comput. Mater. 4 (2018) 53.

[22] X. Li, A. Wang, K.R. Lee, Tribo-induced structural transformation and lubricant dissociation at amorphous carbon/alpha olefin interface, Adv. Theory Simul. 1800157 (2018) 1–10.

[23] X. Li, A. Wang, K.R. Lee, Insights on low-friction mechanism of amorphous carbon films from reactive molecular dynamics study, Tribol. Int. 131 (2019) 567–578.

[24] S. Plimpton, Fast parallel algorithms for short-range molecular dynamics, J. Comp. Phys. 117 (1995) 1–19.

[25] X. Li, P. Ke, H. Zheng, A. Wang, Structure properties and growth evolution of diamond-like carbon films with different incident energies: a molecular dynamics study, Appl. Surf. Sci. 273 (2013) 670–675.

[26] H.J.C. Berendsen, J.P.M. Postma, W.F. van Gunsteren, A. DiNola, J.R. Haak, Molecular dynamics with coupling to an external bath, J. Chem. Phys. 81 (1984) 3684–3690.

[27] Y. Mo, K.T. Turner, I. Szlufarska, Friction laws at the nanoscale, Nature 457 (2009) 1116–1119.

[28] L. Pastewka, S. Moser, M. Moseler, Atomistic insights into the running-in, lubrication, and failure of hydrogenated diamond-like carbon coatings, Tribol. Lett. 39 (2010) 49–61.

[29] G. Zilibotti, S. Corni, M.C. Righi, Load-induced confinement activities diamond lubrication by water, Phys. Rev. Lett. 111 (2013) 146101.

[30] S. Bai, H. Murabayashi, Y. Kobayashi, Y. Higuchi, N. Ozawa, K. Adachi, J.M. Martin, M. Kubo, Tight-binding quantum chemical molecular dynamics simulations of the low friction mechanism of fluorine-terminated diamond-like carbon films, RSC Adv. 4 (2014) 33739–33748.

[31] H. Lan, T. Kato, C. Liu, Molecular dynamics simulations of atomic-scale tribology

between amorphous DLC and Si-DLC films, Tribol. Int. 44 (2011) 1329–1332.

[32] G.T. Gao, P.T. Mikulski, J.A. Harrison, Molecular-scale tribology of amorphous carbon coatings: effects of film thickness, adhesion, and long-range interactions, J. Am. Chem. Soc. 124 (2002) 7202–7209.

[33] S. Bai, T. Onodera, R. Nagumo, R. Miura, A. Suzuki, H. Tsuboi, Terminated diamond-like carbon films investigated by molecular dynamics and quantum chemical calculation, J. Phys. Chem. C 116 (2002) 12559–12565.

[34] G.T. Gao, P.T. Mikulski, G.M. Chateauneuf, J.A. Harrison, The effects of film structure and surface hydrogen on the properties of amorphous carbon films, J. Phys. Chem. B 107 (2003) 11082–11090.

[35] K. Hayashi, K. Tezuka, N. Ozawa, T. Shimazaki, K. Adachi, K. Momoji, Tribochemical reaction dynamics simulation of hydrogen on a diamond-like carbon surface based on tight-binding quantum chemical molecular dynamics, J. Phys. Chem. C 115 (2011) 22981–22986.

[36] G. Kresse, J. Furthmüller, Efficiency of ab initio total energy calculations for metals and semiconductors using plane-wave basis set, Comput. Mater. Sci. 6 (1996) 15–50.

[37] G. Kresse, J. Furthmüller, Efficient iterative schemes for ab initio total-energy

calculations using a plane-wave basis set, Phys. Rev. B 54 (1996) 11169–11186.

[38] L. Cui, Z. Lu, L. Wang, Probing the low-friction mechanism of diamond-like carbon by varying of sliding velocity and vacuum pressure, Carbon 66 (2014) 259–266.

[39] E. Rabinowicz, Friction and Wear of Materials, second ed., John Wiley & Sons, New York, 1995.

[40] Y.N. Chen, T.B. Ma, Z. Chen, Y.Z. Hu, H. Wang, Combined effects of structural transformation and hydrogen passivation on the frictional behaviors of hydrogenated amorphous carbon films, J. Phys. Chem. C 119 (2015) 16148–16155.

[41] T.B. Ma, L.F. Wang, Y.Z. Hu, X. Li, H. Wang, A shear localization mechanism for lubricity of amorphous carbon materials, Sci. Rep. 4 (2014) 3662.

[42] X. Li, A. Wang, K.R. Lee, Comparison of empirical potentials for calculating structural properties of amorphous carbon films by molecular dynamics simulation, Comput. Mater. Sci. 151 (2018) 246–254.

[43] D.R. McKenzie, D. Muller, B.A. Pailthorpe, Compressive-stress induced formation of thin-film tetrahedral amorphous carbon, Phys. Rev. Lett. 67 (1991) 773–776.

[44] T.B. Ma, Y.Z. Hu, H. Wang, Molecular dynamics simulation of shear-induced graphitization of amorphous carbon films, Carbon 47 (2009) 1953–1957.